Porosity engineering of polymeric foams by localised sonication

PACS: 43.35-c

Torres-Sanchez, Carmen; Corney, Jonathan

School of Engineering and Physical Sciences, Mechanical Engineering, Heriot-Watt University. Edinburgh. EH14 4AS. United Kingdom; c.torres@hw.ac.uk

Abstract

A variety of materials require functionally graded cellular microstructures whose porosity is engineered to meet specific applications (e.g. polymer and/or ceramics that mimic biological material -soft tissue, bone; structural polymers - foams- with specific mechanical, thermal properties, etc). Although many foams can be manufactured with homogenous porosity, there are no generic processes for controlling the distribution of porosity within the resulting matrix. Motivated by the desire to create a flexible process for engineering heterogeneous foams, the authors have investigated how ultrasound, applied during the foaming stages of a polyurethane melt, affects its cellular structure and the distribution of the pore size. The experimental results demonstrated how ultrasound exposure (for a given frequency and acoustic pressure) influenced the volume and distribution of pores within the final polyurethane matrix: the data demonstrates that porosity (i.e. volume fraction) varies in direct proportion to the acoustic pressure magnitude of the ultrasound signal. The effects of ultrasound on porosity demonstrated by this work offer the prospect of a manufacturing process that can adjust the cellular geometry of foam and hence ensure that the resulting characteristics match the functional requirements.

1. INTRODUCTION

Optimum performance and synergetic features of manufactured engineering components could be achieved if the local porosity of foamed materials could be controlled. Mechanical, electrical, thermal and structural properties are directly linked to density distribution (i.e. content and location of voids) [1]. The need for heterogeneous cellular materials has been widely recognised [2, 3]. However, there is not a fully developed manufacturing technology that allows the design of these components and permits the tailoring for functionalities (i.e. porosity gradation) in fields such as thermal and electrical technology, filtration, drug release and manufacturing of biomaterials for scaffolding and orthopaedic use [4, 5].
The structure of a foam is characterised by the distribution, size and wall thickness of cells in the bulk material. These features are the result of many factors (e.g. temperature, pressure, reactants concentrations, etc) some of which are known to be affected by ultrasonic irradiation.

The aim of the work reported here is to investigate the feasibility of varying the structure of cellular foams through precisely measured and localised application of ultrasound during the foaming process. The effects investigated are illustrated in **Figure 1a, 1b and 1c**, which shows a cross-section of three foams irradiated at different locations using the same acoustic pressure. It can be seen that the gradation of porosity of foam 1a and 1c is inverted in foam 1b.

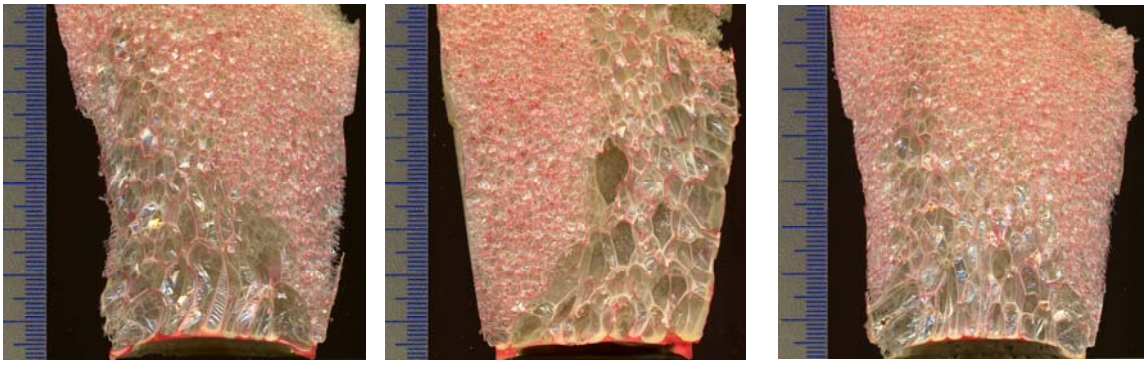

Figure 1: Cross-section of foams sonicated at different distances from the probe but same acoustic pressure (irradiating source was located on the left of these cross-sections)

This paper is structured as follows: section 2 briefly outlines chemical and ultrasonic principles underlying the sonochemistry process described; section 3 introduces the experimental procedure; section 4 presents the results and section 5 discusses the wider significance of the findings before some conclusions are drawn in section 6.

2. BACKGROUND

2.1 Polymeric Foams

Foam is the dispersion of a gas in a liquid, which creates a characteristic structure when the matrix solidifies. Once cured, the foam consists of individual cells, or pores, the walls of which have completely polymerised and solidified to form a skeletal structure. For some polymeric foams, there might exist a latter stage at which those walls break, leaving an open structure of interconnected pores (flexible complexion). The polyurethane formulation used in this study was not taken further, so the structure remained close-celled after curing (rigid structure) [6]. The chemical reaction that occurs between polyols and diisocyanate group to produce polyurethane [7, 8] with distilled water employed as a blowing agent is:

HO-R-OH (**polyol**) + O=C=N-R'-N=C=O (**diisocyanate group**) → -O-R-O-CO-NH-R'-NH-CO- (**PU**) + CO_2 (**gas**)

The water diffuses between the chains of polyurethane (**PU**) reacting at the same time with the isocyanate groups at the end of the chains, causing the reticulation, or cross-linking, of the polymer, and forming a rigid solid.

2.2 Ultrasound as a porosity-tailoring agent

Literature has widely reported ultrasonic irradiation to foams under a myriad of specific applications. Among others, the interaction ultrasound-foam enabled defoaming in bottling of fizzy drinks and the dissipation of foam in reaction/fermentation vessels [9, 10], controlled polymerisation rate [11], assisted in the removal of contaminants [12], aided food dehydration [13] and drug delivery [14]. Many of these applications exploit the ultrasonically stimulated *transient-cavitation* effect (rapid growth and explosive collapse of microscopic). An established research trend focusing on irradiation of foams under *stable-cavitation* conditions (i.e. rectified diffusion that enlarges the size of the bubble in a sustainable way) has not been found in the literature.

When bubbles of initial small radii suffer alternate expansion/contraction due to the sinusoidal nature of the soundwave field, under conditions of *stable-cavitation,* this process is positive. Expansions are bigger than contractions and the bubble growth is in resonance with the soundwave and sustained in time. Bubble dynamics play an important role in pore enlargement, but other processes also enhanced by ultrasound (i.e. diffusion and mixing) will influence the dynamics of the process of foam formation. Particularly important in the context of foams and other high viscosity fluids is the ability of ultrasound to produce an increase in mass transport due to diffusion variation [15]. Essentially, sound affects the viscosity of fluids significantly (usually decreasing their viscosity), so acoustic radiation reduces the diffusion boundary layer, increases the concentration gradient and may increase the diffusion coefficient. In addition, turbulent convection provoked by ultrasound decreases the thickness of the mass transfer boundary layer, i.e. the wall of the pore, and increases transport through the membrane. However, if the shear forces provoked by ultrasound are excessive, some cells might rupture affecting the viscoelastic equilibrium in the matrix and, in extreme conditions, leading to a foam collapse (effect of *transient-cavitation*).

The authors have established that it is possible to modify the behaviour of foaming processes (and so the porosity) with the application of ultrasound [16]. This paper extends that work by reporting how the ultrasonic environment influences the local cellular structure (i.e. porosity distribution) of the resulting material.

3. EXPERIMENTAL INVESTIGATION

To enable a systematic investigation of the effect of ultrasound on the formation and final porosity distribution of polyurethane foam, samples were irradiated in a temperature controlled (313K ±1K) water bath over a fixed value of frequency and acoustic pressure. The procedure followed is summarized as follows: 1. A measured amount of reactant was placed in the container located at a certain distance from the sonotrode; 2. The process was initiated by addition of water (the chemical blowing agent and catalyst for the reaction); 3. Ultrasound of known acoustic pressure value was applied; 4. On completion of the reaction, the foam was left to cure for 48hours; 5. Once the sonicated foams were fully cured, they were de-moulded and cut in half with a coarse-tooth saw and the cross-sections scanned for further analysis.

The schematic shown in **Figure 2** illustrates the ultrasonic source and the polypropylene container (material chosen for its similar acoustic impedance to water) that holds the reactants (5cm diameter, 7cm height, 0.16mm thickness) within the water bath (lined to minimise ultrasonic reflection). The use of water bath ensured the temperature of the environment could be controlled independently of the effects of ultrasound. The container was firmly clamped with a lab stand and positioned along the longitudinal axis of the bath. The ultrasonic piezoelectric source used (a Bandelin Sonopuls sonotrode, Germany, UW 3200) irradiated at 20kHz. The applied power to the transducer varied depending on the location of the vessel and more details can be found in section 4. In order to have both transducer and receiver aligned, the sonotrode tip was immersed 2 cm below the free surface, on the same plane that central plane of the container.

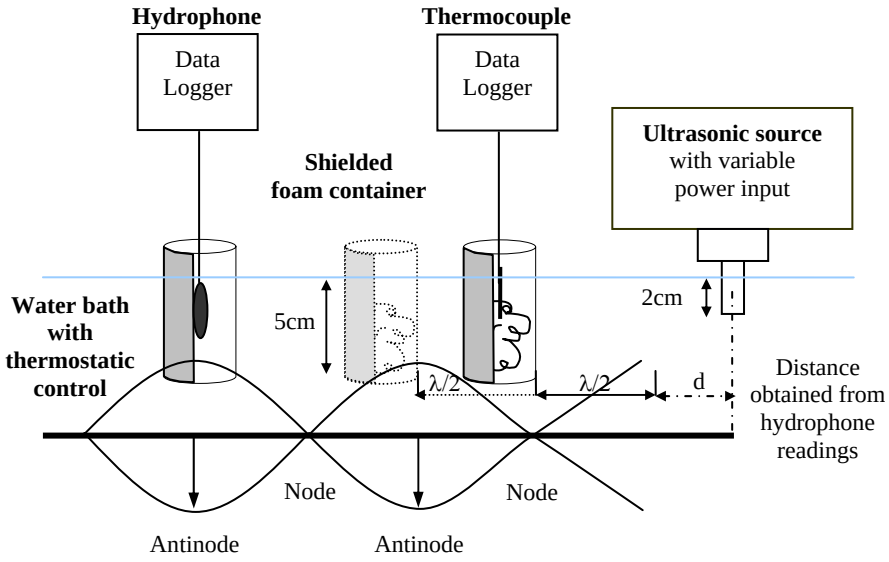

Figure 2: Schematic of the experimental rig with a representation of sonic field (mapped by hydrophone)

Experimental chemicals: The reactants used in this study (Dow Europe GmbH, Switzerland) were pre-treated and the diisocyanate content in the mixture was rectified to have a fixed 40%. The amount of distilled water added was directly related to that amount (20%vol H_2O per ml mixture). This was done using the same procedure of stirring at a standard time of 70 seconds and minimising air intake into the mixture. All mixtures were sonicated in an open-vessel container to avoid the build up of the internal pressure due to the water vapour and gases (e.g. CO_2) generated by the reaction that could provoke unwanted implosion of bubbles. Containers faced perpendicularly the sonicating probe and had the opposite 180° of their surface shielded by absorbent material to minimise reflections from the walls and enable investigation of the effects by "direct" 'near field' sonication. Thermocouples were held in the middle of the mixture and used to monitor the reaction and establish its completion (i.e. after peak temperature).

Method: The vessel was placed inside the bath along the sine wave (detected by the hydrophone) irradiated from the transducer. The 20-minute irradiation period was an off/on cycle of 2min on/1min off starting after adding the distilled water, and then left in the bath for 30minutes until the foam was rigid. This cyclic irradiation was established by initial experimentation as sufficient to induce changes in the foam structure without causing collapse. The ultrasonic irradiation characteristics were established by previous mapping of the ultrasonic bath using a needle-type hydrophone (Brüel&Kjær, Denmark, type 8103) shielded with a barrier made of the same open-vessel material for representative values. The hydrophone also assisted in locating the point of maximum amplitude for acoustic pressure nearby the transducer's horn and showed as well the partial maxima of pressure amplitude values at odd multiples (i.e. 1, 3, 5, 7) of a half-wavelength predicted by the sine propagation wave [17].

As the ultrasound signal attenuates (i.e. reduces in amplitude) as it progresses through the water due to viscous loss [18], the intensity of the ultrasound signal will vary from point to point within the bath. For this experimental series, the input power to the transducer was varied in order to adjust the acoustic pressure at each of the locations of the vessel and maintain it within a tolerance range. The wavelength value for a soundwave of 20kHz is 7.4cm. Therefore, at a half-wavelength (i.e. 3.70cm) distance from the point of maximum pressure amplitude, and at its odd multiples (i.e. 1, 3, 5, etc) a node will appear. Nodes are locations at which value for the energy is zero, amplitude equals to zero. Antinodes (places of maximum energy, when amplitude is maximum) will appear at the even multiples (i.e. 2, 4, 6, etc).

4. QUANTIFYING POROSITY DISTRIBUTION IN POLYURETHANE FOAMS

The density of a cellular solid has been defined [19] as the ratio of the density of the foam to the density of the solid material (ρ^*/ρ_s). The density of a foam is indicative of its porosity. To assess the effects of the ultrasound exposure on the foam's cellular structure, a method of characterising the porosity distribution within a material is essential. For open-cell structures (e.g. flexible foams, rocks), porosity can be measured using liquid displacement techniques (e.g. Arquimedes', toluene infiltration displacement, mercury-porosimetry), which provide an average density value for the bulk material (e.g. measurement permeability and tortuosity in a sample). However, for this work, closed-pore foams were manufactured and these methods were not applicable. Instead, each sample was sliced and the porosity assessed using digital image analysis. Similar structure characterisation methods have been already used in aqueous and polymeric foams [20].

Within the sliced samples, the 3D network of the foam structure can be clearly observed (**Figure 1.a, 1.b and 1.c**). The samples were scanned at 1500dpi resolution in an EPSON Perfection Scanner 1640SU. To allow analysis of the porosity of the heterogeneous sonicated foams and delineation of porous formation, an image analysis application was developed using MatLab™. The purpose was to correlate the topographic distribution of isolines of density in each sample with the manufacturing features of it (e.g. sonicating irradiation, frequency and relative position in the sonicating field). In essence, the program calculated the amount of cell wall material in different areas of a cross section of the foam. Points with the same range of porosity were connected by curves in the same way that contour lines in a topographic map connects continuous points of the same altitude. These topographic maps of porosity provided information on the porosity distribution within a foam cross-section, indicating relative positions of areas with equivalent porosity. In order to isolate the surface plane, the RGB colours for colour of the foam matrix were filtered from the image. Colour power, colour threshold and intensity were also used for a fine tuning. Using this filtered image, a grid was applied to the image, which counted the pixels and adapted (i.e. reduced or expanded) the size of squares in the grid until they matched a given value of intensity. This intensity was set via the mesh spacing initially chosen so it reflected the observed distribution of cellular porosity. The image was then pixelated, so each grid contained a value which was the number of pixels contained in that area. Applying the "contour" option, a set of curves, isolines, was obtained and those joined together all points of equal number of pixels, which was indirectly related to porosity and directly linked to density.

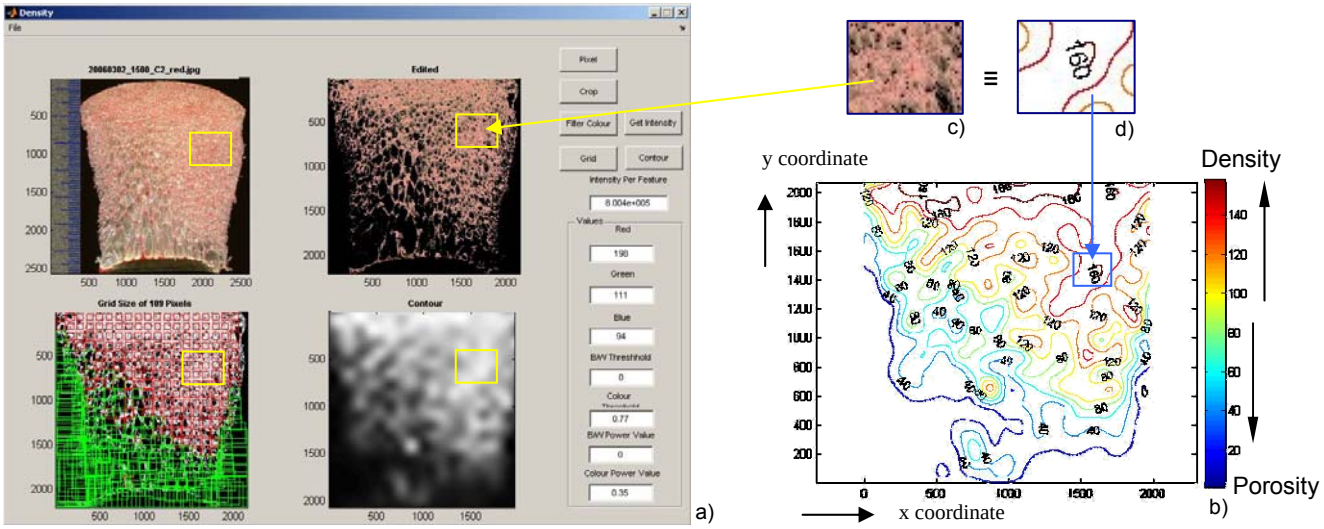

Figure 3: a) MatLab™ Interface; b) isoporosity contour lines; c and d) correspondent areas in image analysis and contour lines

The results were topographic pictures, where points of equal porosity are joined by contour lines. The relative position of the contour lines gave information about the rate of change within an image. Based on the ratio ρ^*/ρ_s, the contours effectively mapped porosity distribution where a value of 200 was set to be equivalent to the density of solid polyurethane. For areas where the colour was red or intense red, the density was higher, so porosity low. For areas where colour was blue, porosity was higher. For areas with no lines, or spaces between lines, there was no variation of porosity in the samples (given the interval used to generate the plot). For example, when foam occupied 80% of the total volume, the value of the lines was 160, as shown in **Figure 3c and 3d**. By using the same parameters for colour filters and threshold, a comparative study among samples could be made.

A cross-section of the topographic profile was created by recording values parallel to a y-axis which was aligned to the irradiation plane of sonication (i.e. aligned with the horn tip). This allowed comparison of porosity gradient among different foams. These curves were analysed using the trapezoidal rule for numeric integrals. In order to quantify the topographic profiles in a way that both location and value could be linked, the negative[1] of the second degree of Legendre's polynomial sequence[2] was applied. This formula characterised both the area under the graph (cross-section) and its distribution. So, although two graphs might have contained the same area, the value of the Legendre's polynomial reflected if more area is contained under the left or right end of the plot.

---

[1] The ultrasonic transducer was located at the left of the samples' cross-section.

[2] $\int_{x_1}^{x_2} P_i(x) \cdot f(x)dx = \int_{x_1}^{x_2} (-1) \cdot x \cdot f(x)dx$ when $i = 1$

4. RESULTS

The output of the investigation on porosity distribution as a function of location of the sample in the bath is present here. The selected power applied to the transducer for this series of experiments was tuned in order to obtain an equal value of acoustic pressure (i.e. signal magnitude, amplitude) when the distance from the transducer to the vessel's wall varied. The acoustic pressure was 18000 Pa (12% tolerance) for 20kHz.

The foams were sonicated at known distances from the maximum acoustic pressure detected immediately near the probe. The chosen distances for this experiment were: 0cm (vessel wall located at the maximum, antinode), at 3.7cm from the maximum (node) and at 7.4cm from the maximum (antinode). The topographic lines of the plane aligned to the axial plane of sonication (e.g. depth of transducer's tip) were used to characterise the porosity distribution of each sample.

The results presented below belong to the sonicated foams in **Figures 1 a, b and c.** Their topographic surfaces (**Figure 4**) have been extracted using the image processing interface presented above. The correspondent section to the irradiation plane (2.5cm from the free surface) has been isolated (Figure 5) and the weighed numerical integration calculated. Values of porosity distribution versus distance are plotted in Figure 6.

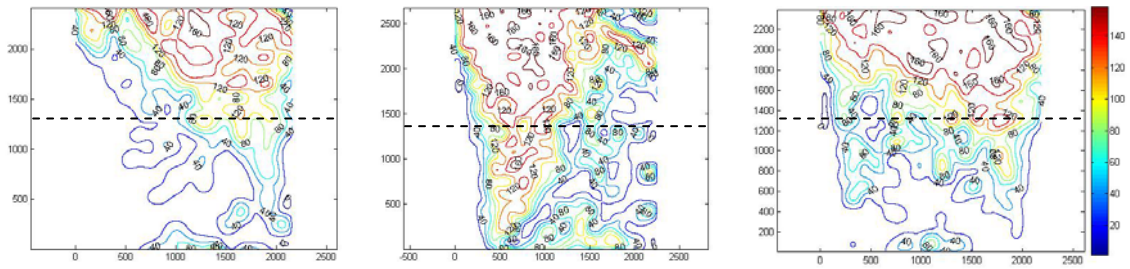

Figure 4: Foams irradiated at same frequency (20kHz) and variable distance from the maximum acoustic pressure: at 0cm, at 3.7cm and at 7.4cm. *(Dashed line represents the irradiation plane for these samples)*

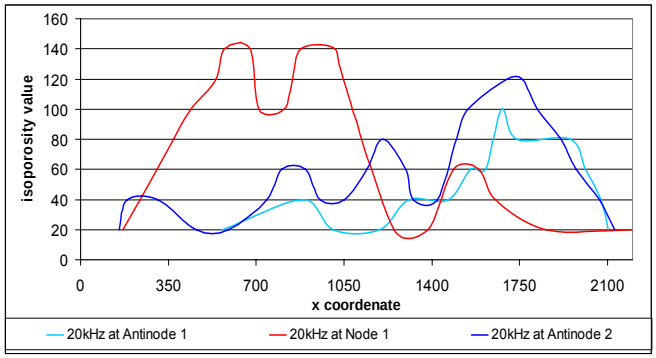

Figure 5: Topographic profiles

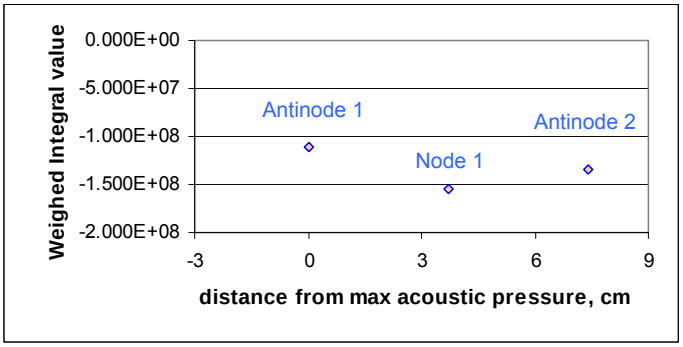

Figure 6: Numeric integral values

5. DISCUSSION

The application of this new technology allows the manufacture of materials with a tailored cellular structure. In this work, polyurethane foams with a controlled orientation and distance to the transducer have been irradiated with ultrasound to produce gradation in porosity.

The volume of the foam exposed to antinodes (points of maximum amplitude of the acoustic pressure) presented higher porosity caused by the formation of larger pores when the mixture was irradiated and its nature was viscoelastic (i.e. liquid to solid transition). In the same way, when the volume was coincident with nodes of the wavefront, that area of the foam presented a small degree of porosity (i.e. density increased). This effect was found to be independent whether the foam was facing the transducer directly, or not (as it can be seen in **Figures 1a, 1b and 1c**).

Due to the nature of the sine wave, antinodes are alternated by nodes. Therefore, for a foam located between an antinode and a node, the porosity gradation was negative, and the distribution was from large to small pores. However, when the foam was located between a node and an antinode, the porosity gradation was positive. It started with small pores that evolved into large pores.

The results from the numeric integral done to the topographic cross-section, and weighed with the negative Legrende's second degree, are presented in **Figure 6**. When comparing values resulting from

foams sonicated at antinodes and nodes, the former presented greater values than the latter. The lack of alignment between values from foams both at antinode position is linked to the attenuation of the signal, which could not be avoided, and it falls within the % of tolerance.
Large values for the numeric integral mean curve (**Figure 5**) was displaced to the right, where large values of 'x coordinate' contribute more, since the ultrasonic transducer was located on the left of the samples' cross-section. Low values are presented by curves displaced to the left, where high values of 'x coordinate' contribute less to the overall integral.
It is thought that the most probable effect that ultrasound provoked in those foams was the mechanical stirring due to ultrasonic excitation.

6. CONCLUSIONS

Localised application of ultrasound with known characteristics of pressure was shown to influence the cellular structure of foamed material in a predictable manner. To do that, the sonication pattern in the field must be known because, depending on the location along the sine wave, the porosity distribution can be varied.
Our experiments have shown that ultrasound can be used to affect local porosity within an specimen using rectified diffusion (i.e. stable cavitation) as a tailoring agent during the foam production. The aim was to show the dependence between the location along the sine wave and the porosity distribution gradation (increasing, positive; or decreasing, negative).
Future work will focus on a deeper investigation of the stable cavitation mechanisms within the foam, so a greater understanding of the cause-effect relationship can be drawn. This would allow a finer adjustment of porosity gradation for a better tailoring of heterogeneity in foams. A more accurate design and shaping of functionally graded materials will open possibilities in the biomedical research (e.g. bio-materials and orthopaedics) where artefacts could be designed 'ad-hoc' to assist in specific requirements.

REFERENCES:

1. Boccaccini, A.R., *Fabrication, microstructural characterisation and mechanical properties of glass compacts containing controlled porosity of spheroidal shape.* Journal of Porous Materials, 1999. **6**(4): p. 369-379.
2. Peng, H.X., Fan, Z., Evans, J.R.G., and Busfield, J.J.C., *Microstructure of ceramic foams.* Journal of the European Ceramic Society, 2000. **20**(7): p. 807-813.
3. van Tienen, T.G., Heijkants, R.G.J.C., Buma, P., de Groot, J.H., Pennings, A.J., and Veth, R.P.H., *Tissue ingrowth and degradation of two biodegradable porous polymers with different porosities and pore sizes.* Biomaterials, 2002. **23**(8): p. 1731-1738.
4. Taboas, J.M., Maddox, R.D., Krebsbach, P.H., and Hollister, S.J., *Indirect solid free form fabrication of local and global porous, biomimetic and composite 3D polymer-ceramic scaffolds.* Biomaterials, 2003. **24**(1): p. 181-194.
5. Yan, Y., Xiong, Z., Hu, Y., Wang, S., Zhang, R., and Zhang, C., *Layered manufacturing of tissue engineering scaffolds via multi-nozzle deposition.* Materials Letters, 2003. **57**(18): p. 2623-2628.
6. Zhang, X.D., Macosko, C.W., Davis, H.T., Nikolov, A.D., and Wasan, D.T., *Role of silicone surfactant in flexible polyurethane foam.* Journal of Colloid and Interface Science, 1999. **215**(2): p. 270-279.
7. Rojas, A.J., Marciano, J.H., and Williams, R.J., *Rigid polyurethane foams: A model of the foaming process.* Polymer Engineering & Science, 1982. **22**(13): p. 840-844.
8. Font, R., Sabater, M.C., and Martínez, M.A., *The leaching kinetics of acetone in an acetone-polyurethane adhesive waste.* Journal of Applied Polymer Science, 2002. **85**(9): p. 1945-1955.
9. Gallego-Juárez, J.A., Rodríguez-Corral, G., Riera-Franco De Sarabia, E., Campos-Pozuelo, C., Vázquez-Martínez, F., and Acosta-Aparicio, V.M., *Macrosonic system for industrial processing.* Ultrasonics, 2000. **38**(1): p. 331-336.
10. Gallego-Juárez, J.A., Rodríguez-Corral, G., Riera-Franco de Sarabia, E., Vázquez-Martínez, F., Acosta-Aparicio, V.M., and Campos-Pozuelo, C. *Development of industrial models of high-power stepped-plate sonic and ultrasonic transducers for use in fluids*. in *Proceedings of the IEEE Ultrasonics Symposium*. 2001.
11. Price, G.J., Lenz, E.J., and Ansell, C.W.G., *The effect of high intensity ultrasound on the synthesis of some polyurethanes.* European Polymer Journal, 2002. **38**(8): p. 1531-1536.
12. Mason, T.J., Collings, A., and Sumel, A., *Sonic and ultrasonic removal of chemical contaminants from soil in the laboratory and on a large scale.* Ultrasonics Sonochemistry, 2004. **11**(3-4): p. 205-210.
13. Mulet, A., Cárcel, J.A., Sanjuán, N., and Bon, J., *New food drying technologies - Use of ultrasound.* Food Science and Technology International, 2003. **9**(3): p. 215-221.
14. Pitt, W.G., Husseini, G., and Staples, B.J., *Ultrasonic drug delivery - A general review.* Expert Opinion on Drug Delivery, 2004. **1**(1): p. 37-56.
15. Floros, J.D. and Liang, H., *Acoustically assisted diffusion through membranes and biomaterials.* Food Technology, 1994. **48**(12): p. 79-84.
16. Torres-Sánchez, C. and Corney, J., *Effects of ultrasound on polymeric foam porosity.* Ultrasonics Sonochemistry, 2007. ***In press***.
17. Kanthale, P.M., Gogate, P.R., Pandit, A.B., and Marie Wilhelm, A., *Mapping of an ultrasonic horn: Link primary and secondary effects of ultrasound.* Ultrasonics Sonochemistry, 2003. **10**(6): p. 331-335.
18. Cheeke, J.D.N., *Fundamentals and applications of ultrasonic waves*. 1st ed. 2002: CRC publisher. 480 pages.
19. Gibson, L.J. and Ashby, M.F., *Cellular solids: structure and properties*. 2nd ed. 1997: Cambridge University Press.
20. Montminy, M.D., Tannenbaum, A.R., and Macosko, C.W., *The 3D structure of real polymer foams.* Journal of Colloid and Interface Science, 2004. **280**(1): p. 202-211.